Alteration of the Optical and Mechanical Characteristics of Cellulose Nanofibre Films Under Thermal Treatment

Ilpo Niskanen (ilpo.niskanen@oulu.fi)
Univeristy of Oulu https://orcid.org/0000-0002-9940-6072
Kaitao Zhang
University of Oulu: Oulun Yliopisto
Henrikki Liimatainen
University of Oulu: Oulun Yliopisto
Shuhei Shibata
Utsunomiya Daigaku
Nathan Hagen
Utsunomiya Daigaku
Rauno Heikkilä
University of Oulu: Oulun Yliopisto
Hidehiko Yoda
Utsunomiya Daigaku
Yukitoshi Otani
Utsunomiya Daigaku

Research Article

Keywords: Nanocellulose, thermal treatment, complex refractive index, birefringence, mechanical properties, thermal stability

Posted Date: June 18th, 2021

DOI: https://doi.org/10.21203/rs.3.rs-589761/v1

Alteration of the optical and mechanical characteristics of cellulose nanofibre films under thermal treatment

Ilpo Niskanen[a], Kaitao Zhang[b], Henrikki Liimatainen[b], Shuhei Shibata[c], Nathan Hagen[c], Rauno Heikkilä[a], Hidehiko Yoda[d], Yukitoshi Otani[c]

[a] Faculty of Technology, Structures and Construction Technology, University of Oulu, P.O. Box 7300, FI-90014 Oulu, Finland

[b] Faculty of Technology, Fibre and Particle Engineering, University of Oulu, P.O. Box 4300, FI-90014, Oulu, Finland

[c] Optical Information Processing and Systems Engineering Division, The Graduate School for the Creation of New Photonics Industries, 1955-1, Kurematsucho, Nishi-ku, Hamamatsu-shi, Shizuoka-ken, 431-1202, Japan

[d] Graduate School of Engineering, Utsunomiya University, 7-1-2 Yoto, Utsunomiya, Tochigi 321-8585, Japan

*) Corresponding author: Ilpo.Niskanen@oulu.fi

Tel: +358 44 3275850

ORCID: 0000-0002-9940-6072

Abstract

Nanocelluloses and their different designs, such as films and nanopapers, have gained considerable interest in many application areas due to their unique properties. For many purposes, such as for packaging and electronics, the thermal stability of nanocellulose materials is a crucial characteristic. In this study, the effects of heat treatment (100ºC, 150ºC and 200ºC) on the optical and mechanical properties of 2,2,6,6-tetramethylpiperidinyl-1-oxy radical-oxidised cellulose nanofibre (TO-CNF) films were investigated, especially the alteration of the colour, complex refractive index and birefringence of the films. Exposing TO-CNF films to high temperatures (> 150ºC) induced permanent transformations in the CNF structure, leading to an increase in the refractive index, decreases in the birefringence and crystallinity index, colour darkening and significant deterioration of the mechanical properties.

Keywords: *Nanocellulose; thermal treatment; complex refractive index; birefringence; mechanical properties; thermal stability*

Introduction

Nanocellulose is a functionalisable renewable biopolymer material that has gained increasing interest for a range of applications relevant to the fields of packaging, technical films and foams, nanocomposites, electronics, photonics, medicines, etc. (Abitbol et al. 2016) and Wang et al. 2019). In the last years, several new biorefinery concepts have been established to produce cellulose nanomaterials at a larger scale, and the nanocellulose market is expected to grow from US$297 million in 2020 to US$783 million in 2025 (Nanocellulose market, 2020). This trend is promoted by the emerging green circular economy based on renewable resources, and by the unique features of nanocellulose, such as its superior mechanical properties, light weight, high surface area, optical transparency, low coefficient of thermal expansion and tailorable chemistry (Pakharenko et al 2021, Gan et al. 2021).

The thermal stability and alteration of the nanocellulose characteristics under high temperatures are relevant for many applications, such as packaging, composites and electronics (Agustin et al. 2016). High temperatures (> 100ºC) can cause changes in the cellulose molecular and crystal structure and can compact the networked structure of cellulose nano-entities. Controlled thermal treatments of solid nanocellulose materials such as films can also be used to improve the mechanical strength (e.g. tensile strength, elongation at break, Young's modulus) (Rubentheren et al. 2016), reduce the water content reduction (Rubentheren et al. 2016) and increase the hardness (Wu et al. 2013) of the films. Typically, the maximum thermal treatment temperature of nanocelluloses is below 200ºC because higher temperatures of 200–300ºC start to degrade the cellulose polymeric structure (Gan et al. 2021).

57 The optical properties of nanocellulose are important parameters for films and
58 nanopapers, and they may also be affected by elevated temperatures (thermal stress)
59 (Pakharenko et al 2021). The optical properties of nanocellulose films have been
60 commonly investigated by analysing the reflection, absorption, scattering or
61 polarisation of light to obtain different variables, such as transmittance (Sun et al.
62 2018), complex refractive index (Niskanen et al. 2019b), optical activity (Zlenko et
63 al. 2019), colour (Vardanyan et al. 2015), birefringence (Orellana et al. 2018),
64 opacity (Zhu et al. 2011), and gloss (Kong et al. 2019). The knowledge of the
65 transformation of the optical characteristics of nanocellulose materials as a function
66 of temperature is still incomplete, and the previous studies have mainly addressed
67 the colour of cellulose nanomaterials (Pakharenko et al 2021). It has been found
68 that the values of the colour differences and transmittance increase, and the value
69 of lightness decreases, as a function of the heat treatment temperature. The thermal
70 discolouration has been strongly attributed to the carbonyl and carboxyl functional
71 groups of pure (lining- and hemicellulose-free) cellulose, which can initiate the
72 formation of chromophores especially in the oxidised cellulose nanomaterials such
73 as TEMPO (2,2,6,6-tetramethylpiperidinyl-1-oxy radical) mediated (Ahn et al.
74 2019).

75 In our previous work, we developed a method of determining the complex refractive
76 index of cellulose nanocrystals (CNCs) as a function of wavelength by combining
77 the Beer-Lambert and immersion-matching methods (Niskanen et al. 2019b). The
78 sizes of nanocelluloses (CNCs and CNFs) were in turn analysed using Rayleigh
79 approximation and the Mie theory (Niskanen et al. 2019a). The change in the
80 birefringence properties of the thermally modified wood was obtained by
81 measuring the light reflection with a Stokes imaging polarimeter based on the
82 Mueller matrix method (Niskanen et al. 2020). The present study aimed to

investigate the optical (colour, complex refractive index and birefringence), structure (degree of crystallinity, thermal stability and chemical bonds) and mechanical (tensile strength, strain and Young's modulus) properties of heat-treated films of 2,2,6,6-tetramethylpiperidinyl-1-oxy radical-oxidised cellulose nanofibres (TO-CNFs) and to provide a further understanding of the behaviour of nanocellulose films at elevated temperatures (100–200ºC).

Materials and Methods

Materials

Bleached birch (Betula pendula) chemical wood pulp obtained in dry sheets was used as a cellulose raw material after disintegration in deionised water. The properties of birch pulp were determined in a previous study (Liimatainen et al. 2011). The cellulose, xylan and glukomannan contents of the pulp were 74.8%, 23.6% and 1.1%, respectively. The 2,2,6,6-tetramethylpiperidinyl-1-oxy radical (TEMPO), sodium bromide and sodium hypochlorite solution (NaClO, 15 wt%) were obtained from Sigma–Aldrich (Finland).

Preparation of TEMPO-oxidised CNFs (TO-CNFs)

The cellulose pulp was subjected to TEMPO-mediated oxidation, mechanical delamination treatment and purification. The TEMPO-mediated oxidation was performed as previously described [26]. In the present study, 10 mmol NaClO per gram of pulp fibre was used to achieve a charge density of 1.0 mmol/g. After the oxidation and washing with water (until the conductivity of the filtrate was already below 20 µS/cm), a suspension with a 0.6% dry-matter content was prepared and was delaminated via probe sonication for 1 h (Heilscher UP 400s, 0.5 s power discharge and 0.5 s pause, 60% amplitude and 22 mm probe tip diameter) to obtain

TO-CNFs. To remove the larger fibres and metal dust generated from the sonication probe and to obtain an aqueous TO-CNF suspension, the sample was centrifuged at 8,000 rpm for 10 min.

Preparation of TO-CNF films

TO-CNF films were prepared via casting. The TO-CNF suspension was degassed overnight using vacuum and was then poured into a polystyrene Petri dish and dried with 50% humidity at room temperature for more than 1 week. The obtained self-standing TO-CNF films were heat-treated in an oven for 3 h at 100ºC, 150ºC and 200ºC, respectively. The thicknesses of the TO-CNF films (reference non-treated TO-CNF film and TO-CNF films heat-treated at 100ºC, 150ºC and 200ºC, respectively) measured via scanning electron microscopy were 27.7, 28.2, 27.6 and 28.1 µm, respectively.

Characterisation of the TO-CNF films

Colorimeter

The colour of the TO-CNF films was measured with a spectrophotometer (Lorentzen & Wettre Elrepho 070) under a D65 light source. The colour analysis was based on the CIE 1976 L*a*b* (CIELAB) colour space. The colour was defined by the parameters L* = lightness (or clarity) of the colour (L* = 0 yields black and L* = 100 white), a* = position between magenta and green (green indicates negative values and magenta positive) and b* = position between yellow and blue (blue indicates negative values and yellow positive). The colour difference ΔE between two colour stimuli was calculated as the Euclidean distance between the points representing them in the L*a*b* colour space (Pakharenko et al 2021; Matsuo et al. 2012). The values of ΔE between 0.5 and 1 in colour difference can already be perceived by the human eye. The total colour differences $\Delta E\_ab\hat{} *$ were

calculated using the following formulas:

$$\Delta E^*_{ab} = \sqrt{\Delta L^{*2} + \Delta a^{*2} + \Delta b^{*2}}, \quad (1)$$

where $\Delta L^* = L^* - L^*_0$, $\Delta a^* = a^* - a^*_0$ and $\Delta b^* = b^* - b^*_0$. L^* is a lightness, and a^* and b^* are colour coordinates under the testing conditions. L_0 is the reference value of the lightness and a_0 and b_0 are the reference values of the colour coordinates, respectively.

Spectroscopic photometry

The optical properties of any material can be described by the complex refractive index,

$$N(\lambda) = n(\lambda) - ik(\lambda), \quad (2)$$

where λ is the wavelength, k is the extinction coefficient and n is the real refractive index. The refractive index is defined as the speed of light in a vacuum divided by the speed in the medium. The extinction coefficient (imaginary part) is therefore described as the reciprocal damping of the oscillation amplitude of the incident electric field in the medium (Jackson 1998). The complex refractive index was determined as the absolute (400–1,000 nm) unpolarised reflectance R_0 (λ) and transmission T_0 (λ) spectrally resolved from the TO-CNF films using a Jasco V-670 with an ARMN-735 absolute-reflectance measurement accessory, at a 5° angle of incidence. In mathematical form, this is expressed as

$$R_0 = \frac{(n_0 - n_s)^2 + k^2}{(n_0 + n_s)^2 + k^2} \quad (3)$$

and

$$T_0 = \frac{4\sqrt{n_s^2 + k^2}}{(1 + n_s)^2 + k^2}, \quad (4)$$

where n_0 is the refractive index of the medium, n_s is the refractive index of the film

157 and κ is the extinction coefficient of the film. Generalising this result to the bulk
158 sample polarised reflectance and transmittance R_s and T_s can be defined as
159 shown below

160 $$R_s = R_0 + \frac{T_0^2 R_0 T_v^2}{1 - R_0^2 T_v^2} \quad (5)$$

161 and

162 $$T_s = \frac{T_0^2 T_v}{1 - R_0^2 T_v^2} \quad (6)$$

163 where T_v is the transmittance through the volume. Then T_v can be expressed as

164 $$T_v = exp(-4kd/\lambda), \quad (7)$$

165 where d is the thickness of the film. Using the spectrally resolved bulk sample
166 reflectance and transmission, we estimated the (n, k) model parameters as a function
167 of the wavelength using least-squares fitting to solve the complex refractive index
168 of the film (Macleod 2021; Nilsson 1968).

169

170 *Polarimeter*

171 The retardance (δ) is a measure of the phase shifts when linearly polarised
172 components of light pass through a material. The linear retardance of the TO-CNF
173 films in this study was determined using an Axoscan Mueller matrix polarimeter
174 (Axometrics, USA). The spectra (400–800 nm) were measured at 1.0 nm intervals.
175 The polarisation properties of the TO-CNF films were obtained from the
176 decomposition analysis of the Muller matrix measured by a dual-rotating retarder
177 system, and the polarisation property images were obtained by moving the sample
178 through an XY motor stage (range: 200x200 mm; resolution: 1 mm). The
179 birefringence (Δn) optically anisotropic film is obtained from the expression

$$\Delta n(\mathrm{n}_o - \mathrm{n}_e) = (\delta \cdot \lambda) \,/\, ((2\pi \cdot d)\,), \quad (8)$$

where δ is the retardance, λ is the wavelength, n_o is the ordinary refractive index, n_e is the extraordinary refractive index and d is the film thickness (Smith 2002).

Transmission electron microscopy (TEM)

The morphological features of TEMPO oxidized CNFs (TO-CNFs) were observed by transmission electron microscope (TEM, JEOL JEM-2200FS, Japan). Preparation of the samples was performed by first adding a small droplet of 0.003 to 0.005 wt% nanocellulose suspension on the top of carbon-coated copper grid. After setting for one minute, the sample was absorbed by a small piece of filter paper, the sample left on the grid was negatively stained with uranyl acetate (2% w/v) for 1 min. The staining agent was then removed again by filter paper. The standard conditions with 200 kV were used during the TEM analysis.

Field emission scanning electron microscopy (FESEM)

The FESEM images of the films were obtained using a field emission scanning electron microscope (Zeiss Sigma HD VP, Oberkochen, Germany) at a 0.5 kV acceleration voltage. All the samples were sputtered with platinum before observation.

X-ray diffraction (XRD)

The XRD patterns of the samples were recorded using a Rigaku SmartLab 9 kW XRD machine. The analysis involved the following parameters: $K\alpha$ radiation ($K_{\alpha 1}$ = 1.78892 Å; $K_{\alpha 2}$ = 1.79278 Å; $K_{\alpha 1}/K_{\alpha 2}$ = 0.5) and a scan rate of 3°/min between 10° and 50° 2θ and 0.02°/step size. The crystallinity index (C_{rI}, %) was calculated as shown below.

$$C_{rI}(\%) = \frac{I_{200} - I_{am}}{I_{200}} 100, \quad (9)$$

where I_{200} is the maximum intensity of the principal peak and I_{am} is the intensity of the diffraction attributed to non-crystalline cellulose.

Diffuse reflectance infrared Fourier transform (DRIFT) spectroscopy

Chemical characterisation of the films was carried out using DRIFT spectroscopy. The spectra were recorded on a Bruker Vertex 80v spectrometer (USA) in the 800–4,000 cm^{-1} range with a 2 cm^{-1} resolution.

Thermogravimetric analysis (TGA)

TGA was performed using a thermal analyser (TA Instruments SDT 2960) under nitrogen flow with a constant rate of 60 mL min^{-1}. Each measurement was conducted from 30 to 1,000ºC at a scanning rate of 10 K/min.

Mechanical properties

The mechanical properties (tensile strength, elongation at break and Young's modulus) of the TO-CNF films were determined using a universal testing machine (Zwick D0724587, Switzerland) equipped with a 1 kN load cell. The Young's modulus was obtained by determining the slope of the tensile strength–strain curves. All the samples were cut into 5-mm-wide strips and were placed at 23 ± 1°C with a relative humidity of 50 ± 2% for at least 24 h. The thickness of each specimen was determined using a precision thickness gauge (Hanatek, FT3, St. Leonards-on-Sea, UK), with the average value obtained from three random locations on the sample strip. For the TO-CNF film heat-treated at 200°C, the average thickness of the film before heat treatment was chosen because of the small bubbles that were found on the film surface after 200°C heating. The initial grip separation of the machine was set at 20 mm, and the specimens were tested at a constant crosshead speed of 5 mm/min. At least five specimens were tested, and the

average value obtained was reported.

Results

Colour changes in the thermally modified TO-CNF films

Fig. 1 presents the original, untreated TO-CNF film (reference) and the films heat-treated at 100ºC, 150ºC and 200ºC, respectively, in an oven.

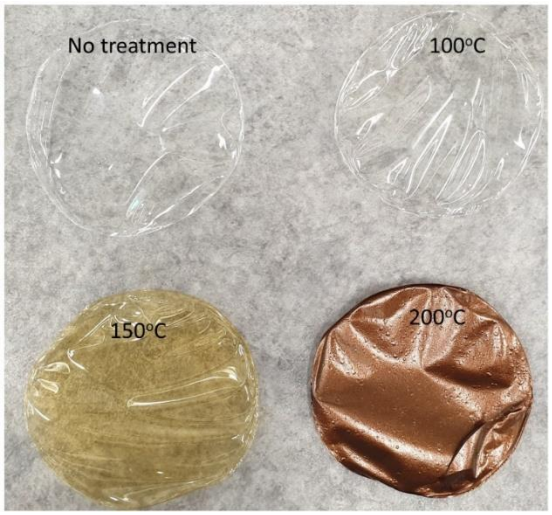

Fig. 1. Reference and heat-treated TO-CNF films (100, 150, 200°C) with 3 h treatment time.

The alteration of the visual appearance of the films heat-treated at 150 and 200ºC was clearly perceived with the naked eye, and the colour of the films changed from transparent to light brown as the heat treatment temperature increased. The yellow or brown film discolouration provided a near-complete UV-blocking ability (Yang et al. 2019). Fig. 2 shows the changes in the total colour difference (ΔE*) of the films. The ΔE* values of the samples heat-treated for 3 h at 100ºC, 150ºC and 200ºC were 1.6, 37.8 and 69.4, respectively; that is, the ΔE* value showed a nonlinear

dependence of the heat treatment temperature, and indicated only minor changes below 100ºC, but notable discolouration was observed at above 150ºC.

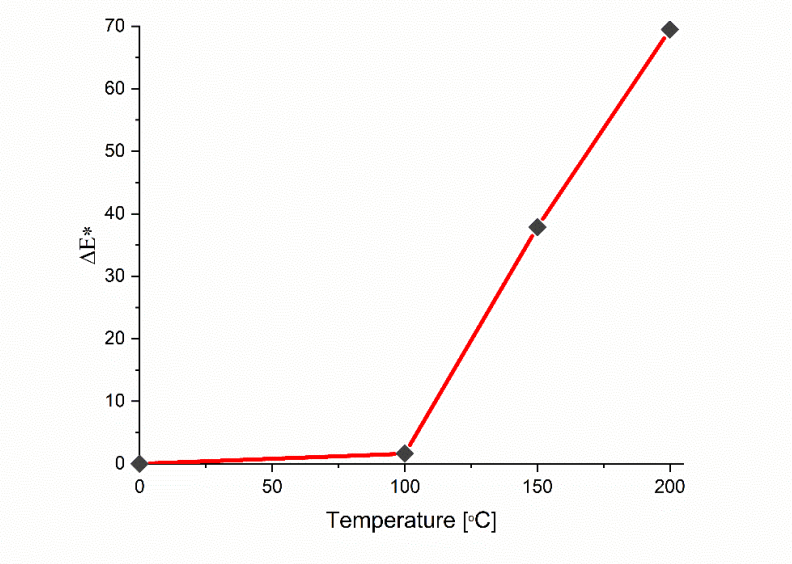

Fig. 2. Changes in total colour difference (ΔE*) of the reference and heat-treated TO-CNF films as a function of treatment temperature.

Previously, thin CNF films produced using only mechanical treatment had ΔE* values of 6.1, 6.6, 7.3 and 10.5 at 80ºC, 120ºC, 160ºC and 190ºC (calculated from the figure), respectively (Pakharenko et al. 2021). Therefore, the TO-CNFs in the current work (charge density: 1.0 mmol/g) were significantly more prone to thermal discolouration. The oxidised groups in cellulose (i.e. CO and COOH) have been generally noted to promote yellowing. In particular, carbonyl groups initiate the formation of chromophores, which are formed later, upon yellowing. Carboxyl groups in turn have a strong synergetic role when carbonyl groups are present, and they promote acidic catalysis and additional activation by electronic effects (Ahn et al. 2019). Especially, the C2 and C3 ketones and aldehyde groups that can be formed due to side reactions have been previously reported to cause brown discolouration for the TEMPO-oxidised nanocellulose (Isogai et al. 2010).

Complex refractive index of the thermally modified TO-CNF films

The influence of heat treatment on the complex refractive index of the TO-CNF films as a function of wavelength is shown in Fig. 3. Fig 3a presents the real effective refractive index spectra of the film samples. The refractive index of untreated CNF had not been previously reported as a function of wavelength; only the value of a single 785 nm wavelength was available, giving a refractive index of 1.458 (Reid et al. 2016). The refractive index estimate obtained by our method was n_{785} = 1.454, matching the literature value very well.

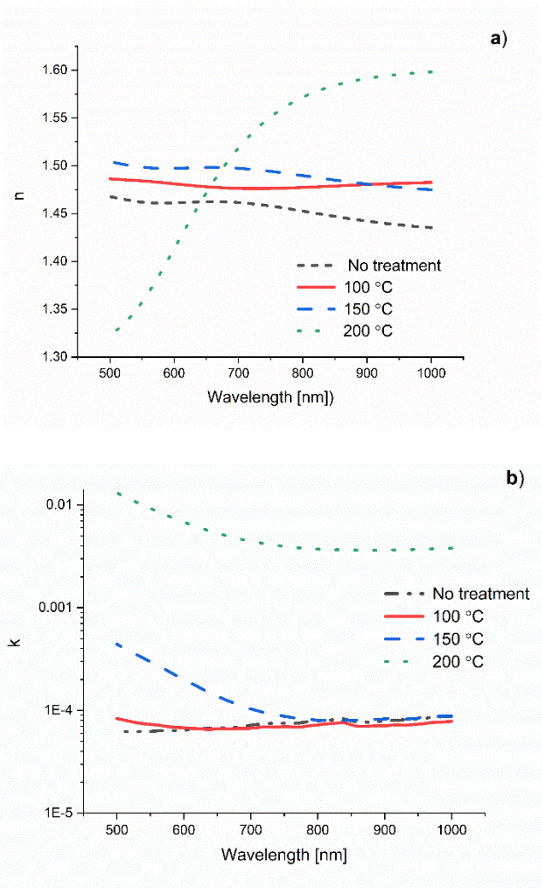

Fig. 3. Real (a) and imaginary (b) parts of the complex refractive indices of the reference and heat-treated TO-CNF films.

The magnitude of the real refractive indices of all the TO-CNF films slightly decreased or stayed at a constant level as a function of the wavelength of light, except that of the film heat-treated at 200ºC (Fig. 3a). This behaviour is attributed to the absorption of the Vis part of incident light for the dark film interface. Hence, in such a case, the light reflection usually becomes weak. The effective refractive indices of the thermally modified TO-CNF films increased as a function of the treatment temperature (Fig 3a). According to these results, the values of the ordinary refractive indices increased with a decrement in the extraordinary refractive index values as the temperature increased.

The same phenomenon was observed earlier for heat-treated pinewood (Niskanen et al. 2012). The refractive indices of original Scots pine and thermally modified wood treated at 180ºC, 200ºC and 230ºC were 1.553, 1.557, 1.587 and 1.596 at 589 nm, respectively, as obtained using the liquid immersion technique. The refractive index of Scots pine treated at 230ºC approached the maximum ordinary refractive index of cellulose (i.e. 1.596 at 589 nm). Similarly, the highest heat treatment (200ºC) of the TO-CNF film resulted in a refractive index of 1.598 at 1,000 nm.

The behaviour of the imaginary part of the complex refractive index curves is shown in Fig. 3b as a function of the wavelength. Significant values of the imaginary part of the complex refractive index were observed only at the higher heat treatment temperatures (150ºC and 200ºC). The reference (untreated) film and the film heat-treated at 100°C had the imaginary part of the refractive index of about 0.0001, without large wavelength dependence. For films, extinction coefficients below 0.0001 are generally considered negligible, and low values of the imaginary component of the complex refractive index correspond to high optical transparency.

306 **Birefringence of the thermally modified TO-CNF films**

307 Fig. 4 shows the spectral dispersion curves of linear retardance and birefringence
308 (Δn) obtained using optical anisotropy. The birefringence decreased with increasing
309 heat treatment temperatures. The birefringence of optically anisotropic materials
310 such as cellulose is considered a measure of the relative area occupied by non-
311 crystalline and crystalline regions (Uetani et al. 2019). The decreasing birefringence
312 with the increase in heat treatment temperature indicating that the birefringence has
313 disappeared. As a result, the structure of CNF has been started to degrade. This
314 influences the mechanical properties of the CNF (Manaf et al. 2016). The
315 birefringence provides information about the whole molecular structure of cellulose
316 whereas XRD mainly provides orientation information about the crystals (Uetani et
317 al. 2019). The birefringence of cellulose measured from bacterial CNF films was
318 previously reported to range from 0.047 to 0.090 (Uetani et al. 2019) depending on
319 the differences in the treatment, state of purity, source, wavelength, measurement
320 temperature and measurement method used. In the present study, the level of
321 birefringence was slightly lower and decreased from approx. 0.035 (reference) to
322 0.075 at the highest heat treatment temperature. Degushi et al. investigated the
323 birefringence of the water suspension of cellulose fibres using an ellipsometer
324 (Degushi et al. 2006). They observed that the birefringence of cellulose is
325 completely lost at 330°C and at a constant pressure of 25 MPa.

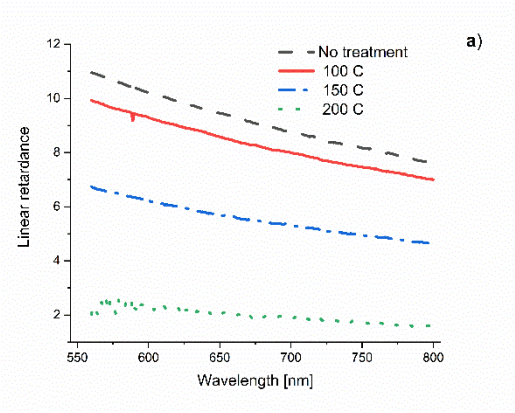

326

327

328 Fig 4. (a) Linear retardance and (b) birefringence of the reference and heat-treated
329 TO-CNF films as a function of the wavelength.

330

331 **Microstructure of the TO-CNF films**

332 Fig. 5 shows the TEM image of TO-CNFs and FESEM images of original TO-CNF
333 and thermal treated TO-CNF films. TO-CNFs are flexible and elongated nanofibrils
334 with an average length ranging from 172 to 958 nm and a width of 5±2 nm. Both
335 the reference (untreated) film and the films heat-treated at 100°C and 150°C,
336 respectively, had a smooth and non-porous surface while small particles and holes
337 were observed on the surface of the film heat-treated at 200°C. These micro- and
338 nano-sized holes probably appeared as a result of the agglomeration of nano-sized
339 cavities between the cellulose molecular chains (Barbash et al. 2016). Moreover,
340 crevices appeared in the cross-section areas and became larger with higher

temperature, indicating notable changes in the microstructure of the nanofibre network.

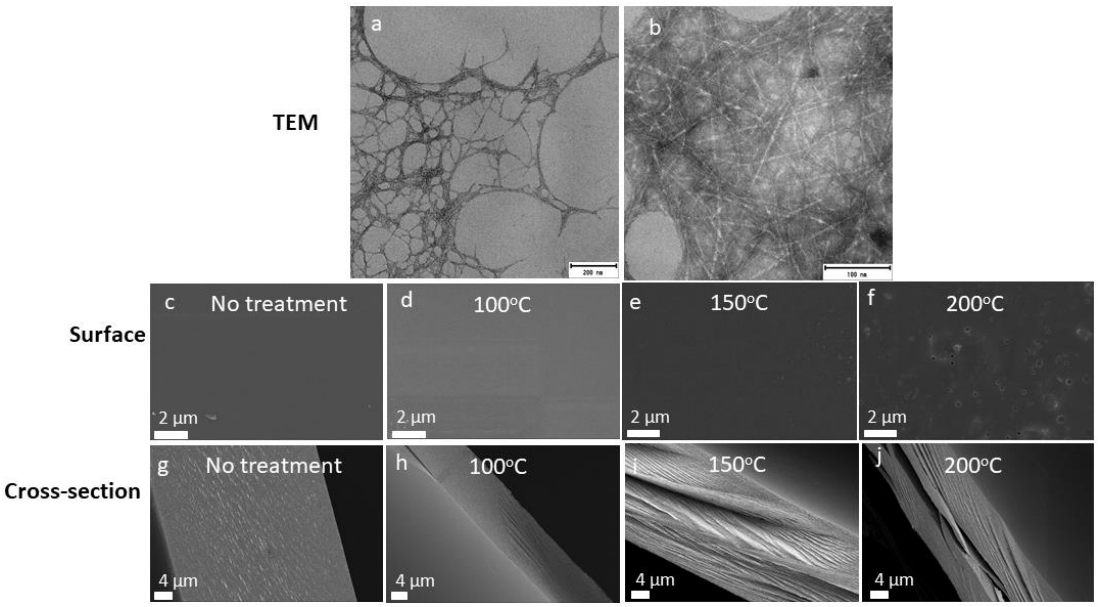

Fig. 5. TEM image of the reference TO-CNF and FESEM images of the surfaces (a–d) and cross-sectional areas (e–h) of the reference and heat-treated TO-CNF films.

Crystalline structure of the thermally modified TO-CNF films

Crystallinity has a significant effect on the physical, optical and mechanical properties of cellulose materials. Fig. 6 depicts the XRD patterns of the films treated at different temperatures in this study. All the films displayed typical cellulose I peaks, with the main 2θ diffraction angles at approximately 18.5 and 26° (Co Kα radiation source) (Selkälä et al. 2016). The results indicated that the crystalline form (allomorph) of the cellulose remained unchanged during the heat treatment. For the films heat-treated at 100°C and 150°C, their crystallinity indices (C_{rI}) decreased only slightly, indicating high crystalline ordering and good stability. However, for the film heat-treated at 200°C, the C_{rI} decreased dramatically (from 58.4 to 45.6%),

358 which was associated with the degradation of the molecular ordering and polymeric
359 structure of cellulose.

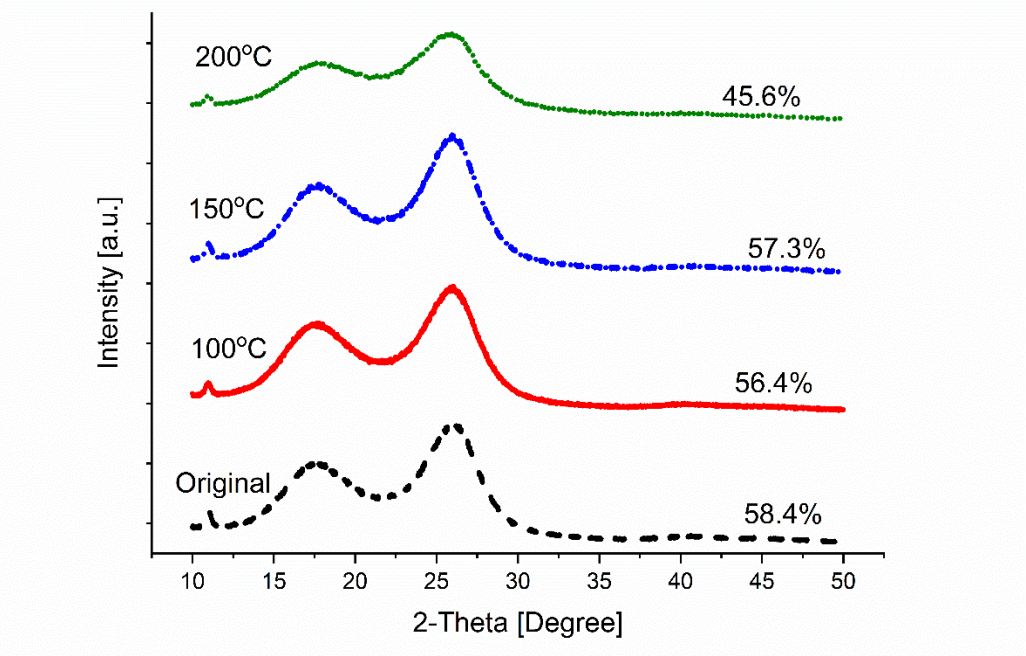

360

361 Fig. 6. X-ray diffractograms and crystallinity indices of the reference and heat-
362 treated TO-CNF films.

363

364 **Chemical analysis of the thermally modified TO-CNF films**

365 Fig. 7 shows the DRIFT spectra of the TO-CNF films in this study. All the DRIFT
366 spectra of the TO-CNF films showed the typical characteristic of cellulose and
367 similar chemical structures. The absorption peaks in the region between 3,350 and
368 3,740 cm^{-1} were O–H stretching vibrations. The peaks at around 2,903 cm^{-1} were
369 associated with C–H stretching vibrations. Notably, the peak at around 1,640 cm^{-1}
370 was the characteristic of the sodium carboxylate group originating from the
371 TEMPO-mediated oxidation. This peak shifted to a lower wavenumber value with
372 a higher heat treatment temperature, which was probably related to the formation
373 of intra- and interfibrillar hydrogen bonds promoted by the heat treatment (Abral et
374 al. 2020). Additionally, a new band at around 1,740 cm^{-1} appeared as the treatment

temperature increased, which was probably ascribed to the carbonyl bonds in chromophore groups formed during the heat treatment (Barbash et al. 2016).

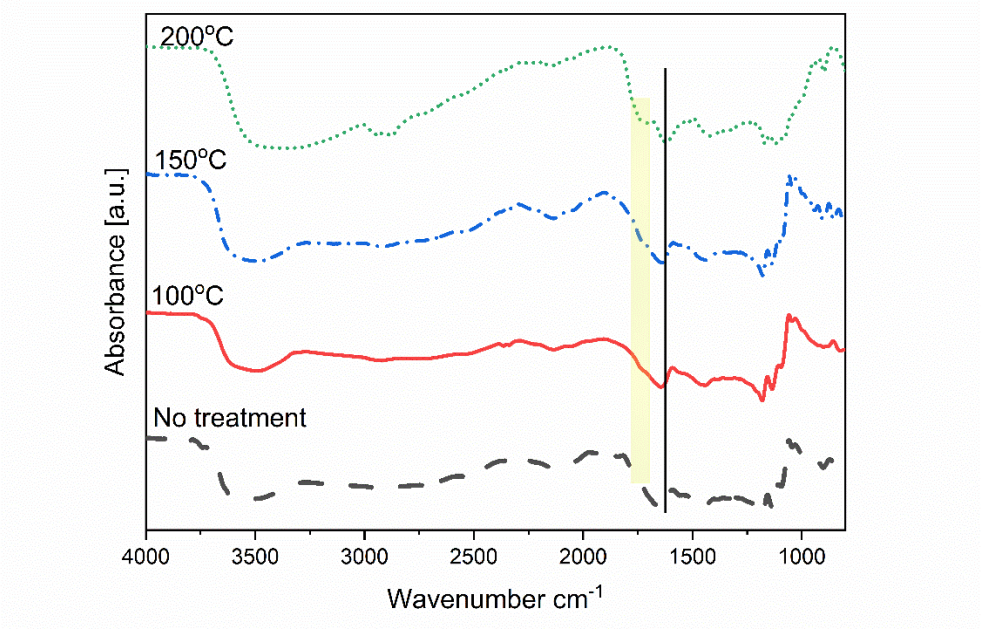

Fig. 7. DRIFT spectra of the reference and heat-treated TO-CNF films.

Thermogravimetric analysis of the thermally modified TO-CNF films

The results of the thermogravimetric analysis of the heat-treated films are shown in Fig. 8. All the films exhibited the typical three weight loss stages of nanocellulosic materials. The weights of all the samples that were heat-treated at temperatures under 200ºC decreased slightly due to the evaporation of the absorbed water. As expected, this water loss decreased as a function of the heat treatment temperature because of the reduction of the residual water in the films. The second weight corresponding to the thermal degradation of the sodium carboxylates started at approximately 200°C. Moreover, it can be noted that the film heat-treated at 200ºC showed a higher thermal degradation point compared to the untreated film. Due to the thermal-oxidative decomposition of the char, a third weight loss was observed when the temperature was higher than 300ºC (Zhao et al. 2013). Additionally, the

amount of char at 1,000ºC was 23.3% for the untreated film, 23% for the film heat-treated at 100ºC, 25.6% for the film heat-treated at 150ºC and 30.2% for the film heat-treated at 200ºC. The higher amounts of char in the heat-treated films were reasonable because the weight loss or decomposition of the films already happened during the heat treatment, before the TG measurement. The temperatures at the maximum weight losses of the reference film and the films heat-treated at 100ºC, 150ºC and 200ºC were determined to be 241.2ºC, 241.6ºC, 241.9ºC and 294.1ºC, respectively. The higher thermal stability of the sample heat-treated at 200ºC can be related to its lower crystallinity, which produces a slow heat transfer ability (Yildirim and Shaler 2017).

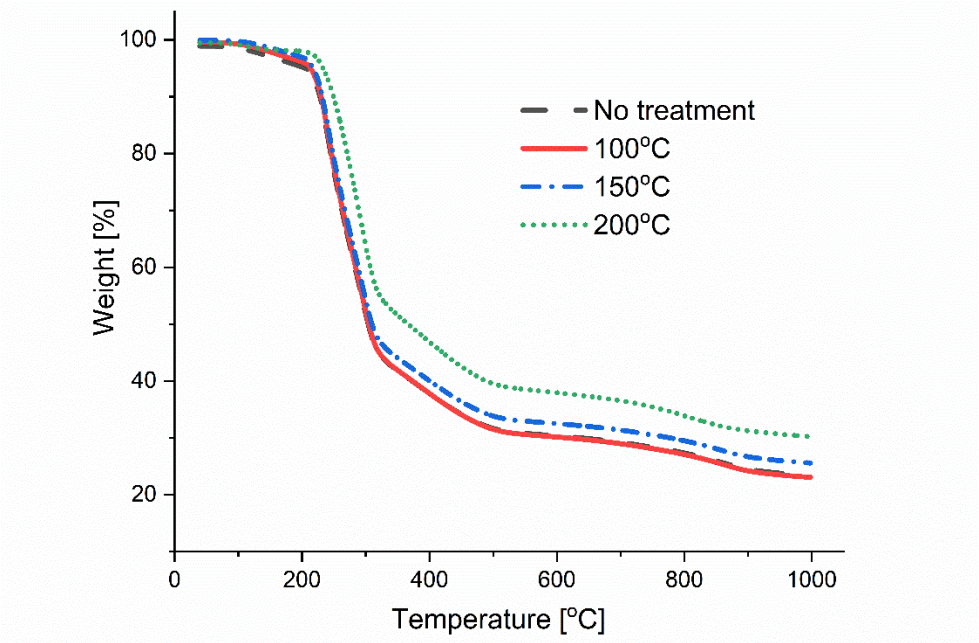

Fig. 8. Weight losses of the reference and heat-treated TO-CNF films.

Mechanical properties of the thermally modified TO-CNF films

The mechanical properties of the TO-CNF films in this study, as measured with the universal testing machine, are presented in Fig. 9. All the TO-CNF films except the film heat-treated at 200ºC were easy to handle and flexible when bent. Both the

tensile strength and the strain displayed a gradual decrease as a function of the heat treatment temperature, already starting at 100ºC. However, the decreases in strength and elongation were small only at 100ºC, when the tensile strength was still > 200 MPa and the strain > 3.5%. At the higher temperatures, the decreases in strength and strain were notable.

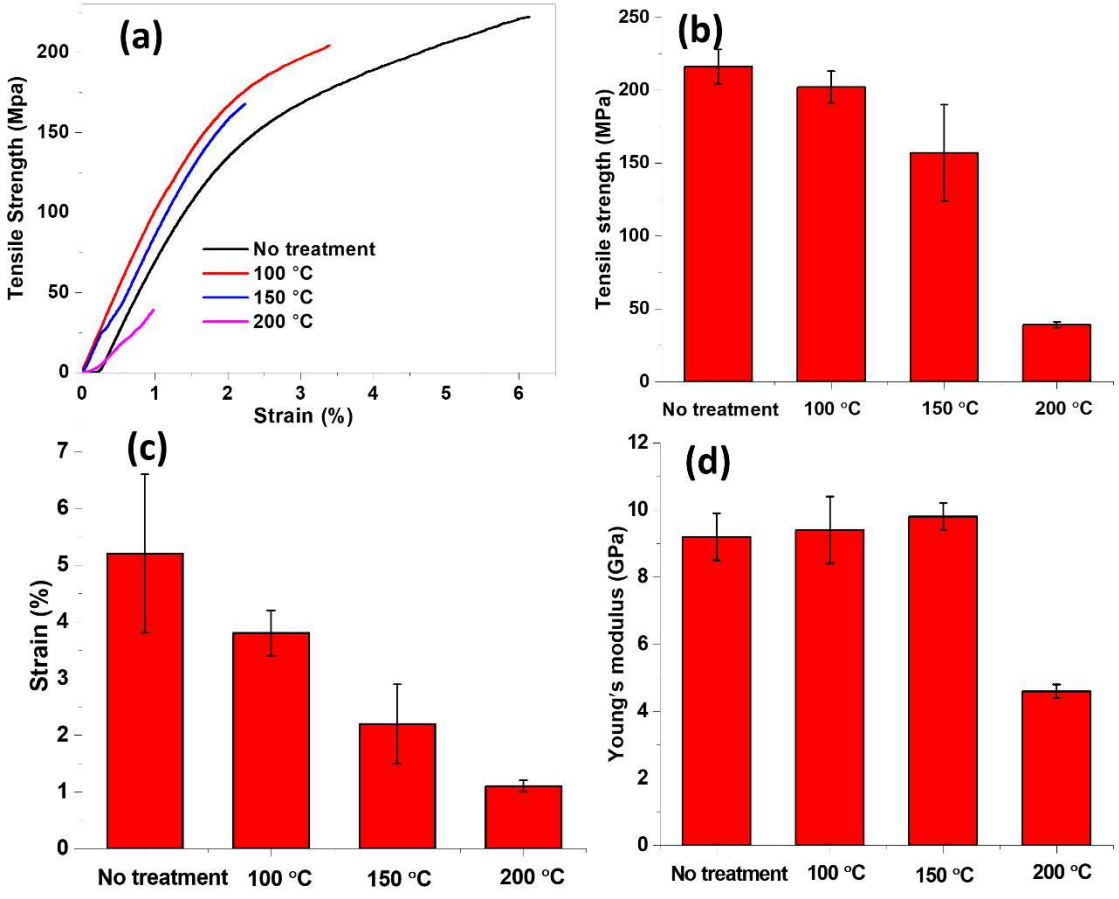

Fig. 9 (a) Typical tensile strength–strain curves and tensile strength (b), strain (c) and (d) Young's modulus of the TO-CNF films heat-treated at different temperatures.

The Young's modulus, in turn, showed a slight increase as a function of the treatment temperature (from 9.2 to 9.8 GPa) until 200ºC. This increase in stiffness can be attributed to the formation of intra- and interfibrillar hydrogen and carbonyl bonds due to the heat treatment (Fig. 7). The TO-CNF film heat-treated at 200ºC

had some small bubbles on its surface, and the film became more brittle and easier to break. Thus, the mechanical properties of the film heat-treated at 200ºC dropped dramatically, and the tensile strength was only 39 ± 2 MPa (82% decrease compared to the reference film), the strain was 1.1 ± 0.1% (79% decrease) and the Young's modulus was 4.6 ± 0.2 GPa (50% decrease). The reduction of the mechanical properties at the higher temperatures was mainly attributed to the decrease in the degree of polymerisation of TO-CNF and to the destruction of the TO-CNF's crystalline structure (Yang et al. 2019), which both decreased the mechanical strength of the individual nanofibres.

Conclusion

The role of thermal stress in the molecular structure of cellulose and nanocellulose is well known and reported in the literature. However, a basic understanding of the optical characteristics of nanocellulose films at elevated temperatures is lacking despite the fact that these are crucial properties in many applications. In the present study, the effects of thermal treatment on the optical, structural and mechanical properties of TO-CNF films were assessed.

The TO-CNF films were colourless at the low heat treatment temperatures (< 100ºC), but significant discolouration was noted at the higher temperatures (> 100ºC). The heat-treated films also showed a significant increase in refractive index. This could have been due to the disappearance of the birefringence of CNF when the temperature increased. The films heat-treated at high temperatures presented lower weight loss in the TG analysis, especially the films heat-treated at 200ºC, but also had a significant decrease in crystallinity. Also, the heat treatment

temperature (> 150ºC) caused a notable decrease in the mechanical strength of the TO-CNF films, and made the films brittle. These factors may limit the suitability of the TO-CNF films for applications, and are presumably affected by the oxidised groups in cellulose (i.e. CO and COOH) formed during TEMPO treatment. Our results provide a deeper understanding of the mechanisms of CNF restructuring after the heat treatment process, and their impact on the optical and mechanical properties of TO-CNF films.

Acknowledgments We gratefully acknowledge funding from Academy of Finland ACNF projects (325276).

Ethics declarations

Human and animal rights This article does not contain any studies with human participants or animals performed by any of the authors.

Conflict of interest The authors declare that they have no conflict of interest.

Availability of data and materials Yes.

References

Abitbol T, Rivkin A, Cao Y, Nevo Y, Abraham E, Ben-Shalom T, Lapidot S, Shoseyov O (2016) Nanocellulose, a tiny fiber with huge applications. Current Opinion in Biotechnology. https://doi.org/10.1016/j.copbio.2016.01.002

Abral H, Ariksa J, Mahardika M, Handayani D, Aminah I, Sandrawati N, Sugiarti E, Muslimin AN, Rosanti SD (2020) Effect of heat treatment on thermal resistance, transparency and antimicrobial activity of sonicated ginger cellulose film. Carbohydrate Polymers. https://doi.org/10.1016/j.carbpol.2020.116287.

Agustin MB, Nakatsubo F,Yano H (2016) The thermal stability of nanocellulose and its acetates with different degree of polymerization. Cellulose. https://doi.org/10.1007/s10570-015-0813-x

Ahn K, Zaccaron S, Zwirchmayr NS, Hettegger H, Hofinger A, Bacher M, Henniges U, Hosoya T, Potthast A, Rosenau T (2019) Yellowing and brightness reversion of celluloses: CO or COOH, who is the culprit?. Cellulose. https://doi.org/10.1007/s10570-018-2200-x

476 Barbash VA, Yaschenko OV, Alushkin SV., Kondratyuk AS, Posudievsky OY, Koshechko V G (2016)
477 The effect of mechanochemical treatment of the cellulose on characteristics of nanocellulose
478 films. Nanoscale Res Lett. https://doi.org/10.1186/s11671-016-1632-1

479 Degushi S, Tsujii K, Horikoshi K (2006) Cooking cellulose in hot and compressed water. Chem
480 Communication. https://doi.org/10.1039/B605812D

481 Gan PG, Sam ST, Abdullah MF, Omar MF (2020) Thermal properties of nanocellulose-reinforced
482 composites: A review. J App. Polym Sci. https://doi.org/10.1002/app.48544

483 Isogai A, Saito T, Fukuzumi H (2010) TEMPO-oxidized cellulose nanofibers. Nanoscale.
484 https://doi.org/10.1039/C0NR00583E

485 Jackson JD (1998) Classical electrodynamics. Willey, New York.

486 Kong L, Xu D, He Z, Wang F, Gu, S, Fan J, Pan X, Dai X, Dong X, Liu B, L, Y (2019) Nanocellulose-
487 reinforced polyurethane for waterborne wood coating. Molecules.
488 https://doi.org/10.3390/molecules24173151

489 Liimatainen H, Sirviö J, Haapala A, Hormi O, Niinimäki J (2011) Characterization of highly
490 accessible cellulose microfibers generated by wet stirred media milling. Carbohydrate Polymers.
491 https://doi.org/10.1016/j.carbpol.2010.11.007.

492 Macleod HA (2021) Thin-film optical filters. CRC Press, Boca Raton.

493 Manaf MEA, Nitta KH, Yamgusci M (2016) Mechanical properties of plasticized cellulose ester
494 films at room and high temperatures. ARPN Journal of Engineering and Applied Science.

495 Matsuo M, Umemura K, Kawai S (2012) Kinetic analysis of color changes in cellulose during heat
496 treatment. J Wood Sci.. https://doi.org/10.1007/s10086-011-1235-5

497 Nanocellulose market (2020), Report code CH3320. https://www.markets
498 andmarkets.com/Market-Reports/nano-cellulose-market-56392090.html (accessed 12 May
499 2021).

500 Nilsson PO (1968) Determination of optical constants from intensity measurements at normal
501 incidence. Appl Opt. https://doi.org/10.1364/AO.7.000435

502 Niskanen I, Forsberg V, Zakrisson D, Reza S, Hummelgård M, Andres B, Fedorov I, Suopajärvi T,
503 Liimatainen H, Thungström G (2019a). Determination of nanoparticle size using Rayleigh
504 approximation and Mie theory. Chemical Engineering Science.
505 https://doi.org/10.1016/j.ces.2019.02.020

506 Niskanen I, Heikkinen J, Mikkonen J, Harju A, Heräjärvi H, Venäläinen M, Peiponen KE (2012).
507 Detection of the effective refractive index of thermally modified scots pine by immersion liquid
508 method. J Wood Sci. https://doi.org/10.1007/s10086-011-1222-x

509 Niskanen I, Räty J, Soetedjo H, Hibino K, Oohashi H, Heikkilä R, Matsuda K, Otani Y (2020)
510 Measurement of the degree of polarisation of thermally modified Scots pine using a Stokes
511 imaging polarimeter. Opt Rev. 178–182. https://doi.org/10.1007/s10043-019-00572-w

512 Niskanen I, Suopajärvi T, Liimatainen H, Fabritius T, Thungström G (2019b) Determining complex
513 refractive index of cellulose nanocrystals by combination of Beer-Lambert and immersion
514 matching methods. Journal of Quantitative Spectroscopy & Radiative Transfer.
515 https://doi.org/10.1016/j.jqsrt.2019.06.023

516 Orellana JL, Wichhart D, Kitchens CL (2018) Mechanical and optical properties of polylactic acid
517 films containing surfactant-modified cellulose nanocrystals. Journal of Nanomaterials.
518 https://doi.org/10.1155/2018/7124260

519 Pakharenko V, Sameni J, Konar S, Pervaiz M, Yang W, Tjong J, Oksman K, Sain M (2021) Cellulose
520 nanofiber thin-films as transparent and durable flexible substrates for electronic devices.
521 Materials & Design. https://doi.org/10.1016/j.matdes.2020.109274

522 Reid MS, Villalobos M, Cranston ED (2016) Cellulose nanocrystal interactions probed by thin film
523 swelling to predict dispersibility. Nanoscale. https://doi.org/10.1039/C6NR01737A

524 Rubentheren V, Ward TA, Chee CY, Nair P, Salami E (2016) Effects of heat treatment on chitosan
525 nanocomposite film reinforced with nanocrystalline cellulose and tannic acid. Carbohydrate
526 Polymers. https://doi.org/10.1016/j.carbpol.2015.12.068

527 Selkälä T, Sirviö J A, Lorite, G S, Liimatainen H (2016) Anionically stabilized cellulose nanofibrils
528 through succinylation pretreatment in urea–lithium chloride deep eutectic solvent.
529 Chemsuschem. https://doi.org/10.1002/cssc.201600903

530 Smith MH (2002) Optimization of a dual-rotating-retarder Mueller matrix polarimeter. Appl Opt.
531 https://doi.org/10.1364/AO.41.002488

532 Sun X, Wu Q, Zhang X, Ren S, Lei T, Li W, Xu G, Zhang Q (2018) Nanocellulose films with combined
533 cellulose nanofibers and nanocrystals: tailored thermal, optical and mechanical properties.
534 Cellulose. https://doi.org/10.1007/s10570-017-1627-9

535 Uetani K, Koga H, Nogi M (2019) Estimation of the intrinsic birefringence of cellulose using
536 bacterial cellulose nanofiber films. ACS Macro Letters.
537 https://doi.org/10.1021/acsmacrolett.9b00024

538 Vardanyan V, Galstian T, Riedl B (2015) Effect of addition of cellulose nanocrystals to wood
539 coatings on color changes and surface roughness due to accelerated weathering. J Coat Technol
540 Res. https://doi.org/10.1007/s11998-014-9634-3

541 Wang Q, Yao Q, Liu J, Sun J, Zhu Q, Chen H (2019). Processing nanocellulose to bulk materials: a
542 review. Cellulose. https://doi.org/10.1007/s10570-019-02642-3

543 Wu Q, Meng Y, Concha K, Wang S, Li Y, Ma L, Fu S (2013) Influence of temperature and humidity
544 on nano-mechanical properties of cellulose nanocrystal films made from switchgrass and cotton.
545 Industrial Crops and Products. https://doi.org/10.1016/j.indcrop.2013.03.032

546 Yang W, Gao Y, Zuo C, Deng Y, Dai H (2019) Thermally-induced cellulose nanofibril films with
547 near-complete ultraviolet-blocking and improved water resistance. Carbohydrate polymers.
548 https://doi.org/10.1016/j.carbpol.2019.115050.

549 Yildirim N, Shaler SA (2017) Study on thermal and nanomechanical performance of cellulose
550 nanomaterials (CNs). Materials. https://doi.org/10.3390/ma10070718

551 Zhao J, Zhang W, Zhang X, Zhang X, Lu C, Deng Y (2013) Extraction of cellulose nanofibrils from
552 dry softwood pulp using high shear homogenization. Carbohydrate Polymers.
553 https://doi.org/10.1016/j.carbpol.2013.05.050

554 Zhu JY, Sabo R, Luo X (2011) Integrated production of nano-fibrillated cellulose and cellulosic
555 biofuel (ethanol) by enzymatic fractionation of wood fibers. Green
556 Chemistry.https://doi.org/10.1039/C1GC15103G

557 Zlenko DV, Nikolsky SN, Vedenkin AS, Politenkova GG, Skoblin AA., Melnikov VP, Michaleva MM,
558 Stovbun SV (2019) Twisting of fibers balancing the gel¯sol transition in cellulose aqueous
559 suspensions. Polymers. https://doi.org/10.3390/polym11050873

Supplementary Files

This is a list of supplementary files associated with this preprint. Click to download.

- Graphicalabstract.pdf
- datafigures.7z